

# Green Chemistry

Accepted Manuscript



This is an *Accepted Manuscript*, which has been through the Royal Society of Chemistry peer review process and has been accepted for publication.

*Accepted Manuscripts* are published online shortly after acceptance, before technical editing, formatting and proof reading. Using this free service, authors can make their results available to the community, in citable form, before we publish the edited article. We will replace this *Accepted Manuscript* with the edited and formatted *Advance Article* as soon as it is available.

You can find more information about *Accepted Manuscripts* in the [Information for Authors](#).

Please note that technical editing may introduce minor changes to the text and/or graphics, which may alter content. The journal's standard [Terms & Conditions](#) and the [Ethical guidelines](#) still apply. In no event shall the Royal Society of Chemistry be held responsible for any errors or omissions in this *Accepted Manuscript* or any consequences arising from the use of any information it contains.



[www.rsc.org/greenchem](http://www.rsc.org/greenchem)

# Specific Immobilization of D-Amino Acid Oxidase on Hematin-functionalized Support Mimicking Multi-enzyme Catalysis

Jian Sun<sup>a</sup>, Kun Du<sup>a</sup>, Xiaoqiang Song<sup>a</sup>, Qian Gao<sup>a</sup>, Hao Wu<sup>b</sup>, Jingjing Ma<sup>a</sup>, Peijun Ji<sup>b</sup>, Wei Feng<sup>a\*</sup>

<sup>a</sup>Department of Biochemical Engineering, <sup>b</sup>Department of Chemical Engineering, Beijing University of Chemical Technology, Beijing, 100029, China

## Abstract

D-amino acid oxidase (DAAO) catalyzes oxidative deamination of D-amino acids to yield corresponding  $\alpha$ -keto acids, producing hydrogen peroxide ( $H_2O_2$ ). D-amino acid oxidase was genetically modified by fusion to an elastin-like polypeptide (ELP). For the enzyme immobilization, multi-walled carbon nanotubes (MWCNTs) were adopted as the model support. MWCNTs were functionalized with hematin. ELP-DAAO was immobilized on the functionalized CNTs by coupling to the hematin. The specific immobilization enabled ELP-DAAO in proximity to the hematin at a molecular distance. The molecular-distance proximity facilitated the immediate decomposition of  $H_2O_2$  catalyzed by the hematin. The evolved oxygen was efficiently utilized to oxidize the reduced cofactor FAD of DAAO, and  $H_2O_2$  was produced. The forming of  $H_2O_2 \rightarrow O_2 \rightarrow H_2O_2$  circle between the DAAO and hematin has been demonstrated to be the driving force to accelerate the deamination reaction. The enzyme kinetics has shown that the ELP-DAAO/hematin-CNTs conjugate exhibited a catalysis efficiency more than three times that of free ELP-DAAO, demonstrating its ability mimicking multi-enzyme catalysis. The methodology for highly specific immobilization of

---

\* Department of Biochemical Engineering, Beijing University of Chemical Technology, Beijing, 100029, China.

E-mail: fengwei@mail.buct.edu.cn.

1 enzyme is not restricted to carbon nanotubes, and can be extended easily to other  
2 micro and nanomaterials as supports for specific immobilization of oxidases.

3 Keywords: D-amino acid oxidase; hematin; immobilization; multi-enzyme

#### 4 **Introduction**

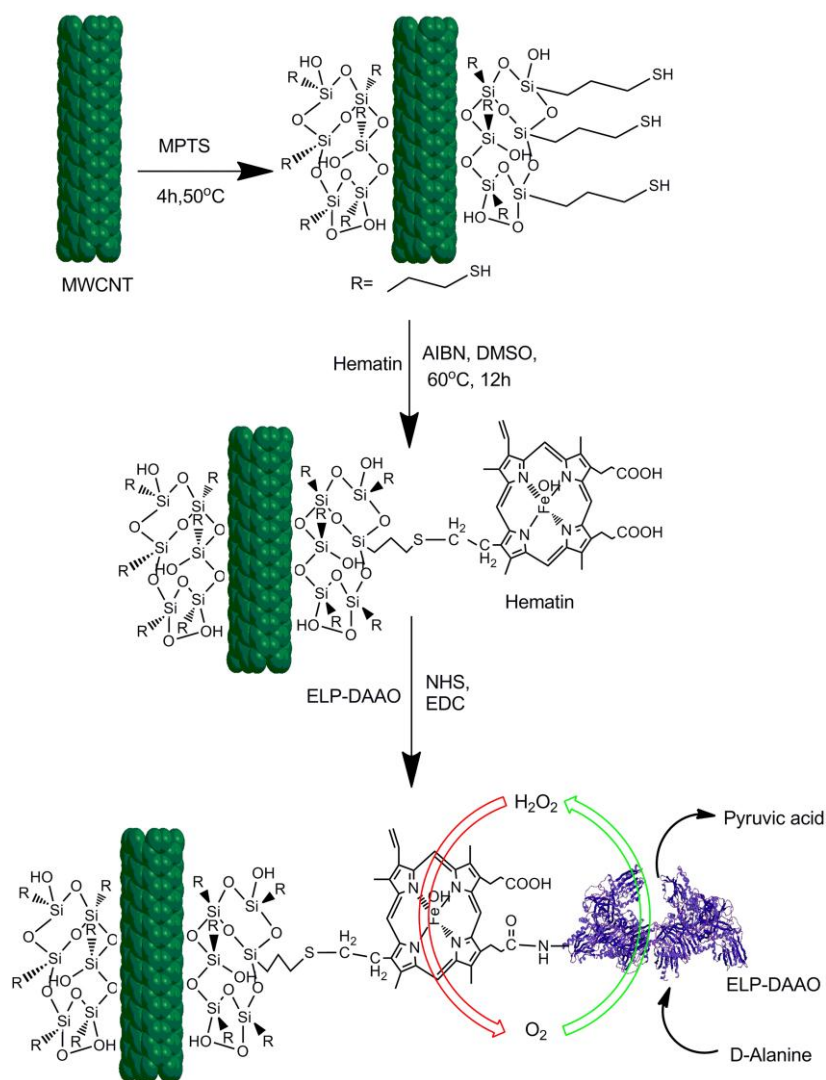
5 Enzymes are "green" biocatalysts and have been utilized to catalyze various  
6 transformations for producing fine chemicals, foods, and pharmaceuticals.<sup>1,2</sup> D-Amino  
7 acid oxidases (DAAOs) are technologically useful flavoenzymes and have been  
8 extensively investigated for use as biocatalysts in industrial applications.<sup>3-6</sup> DAAO  
9 serves as the key enzymes involved in the two-step bioconversion of cephalosporin C to  
10 7-aminocephalosporanic acid, the important intermediate for semisynthetic  
11 cephalosporin antibiotics.<sup>7</sup> Some routes of production of 7ADCA propose that H<sub>2</sub>O<sub>2</sub> is  
12 eliminated.<sup>8</sup> The reactions catalyzed by DAAO can also be used to produce  $\alpha$ -keto  
13 acids from essential D-amino acids,<sup>9,10</sup> to separate racemic mixtures of amino acids,<sup>11</sup>  
14 and to detect and quantify D-amino acids content in foods and in biological fluids.<sup>12-17</sup>  
15 DAAO cooperating with other enzymes can promote the catalysis processes.<sup>18,19</sup> Some  
16 L-amino acid which is obtained through DAAO catalysis is a key intermediate for the  
17 synthesis of pharmaceuticals.<sup>20</sup>

18 D-Amino acid oxidases catalyze the O<sub>2</sub>-dependent transformation of D-amino acid  
19 substrates into the corresponding  $\alpha$ -keto acid, H<sub>2</sub>O<sub>2</sub>, and NH<sub>3</sub>. However, hydrogen  
20 peroxide can induce enzyme deterioration, and DAAO can be partially destroyed in  
21 the presence of hydrogen peroxide.<sup>21, 22</sup> In addition, the evolved hydrogen peroxide  
22 can lead to the by-product inhibition effect on the conversion processes. These two  
23 aspects indicate that accumulation of hydrogen peroxide around the enzyme DAAO  
24 can reduce the catalytic efficiency of the enzyme.<sup>23</sup> To decompose the evolved  
25 hydrogen peroxide, the DAAO catalysis was carried out in the presence of catalase

1 and horseradish peroxidase,<sup>24-26</sup> and catalase was co-immobilized with DAAO on a  
2 support.<sup>10,11, 27, 28</sup> On the other hand, D-Amino acid oxidases are flavoenzymes with a  
3 non-covalently bound flavin adenine dinucleotide (FAD) cofactor. The coenzyme FAD  
4 plays an important role in the activity of DAAO.<sup>29-31</sup> During the catalysis process, the  
5 FAD cofactor is first reduced and subsequently reoxidized by molecular oxygen to  
6 yield hydrogen peroxide. For efficient utilization of molecular oxygen from the  
7 environment, Ghisla et al. investigated O<sub>2</sub> diffusion pathways to enhance reactivity,<sup>32</sup>  
8 Bolivar et al. studied real-time sensing of O<sub>2</sub> availability inside porous carriers to  
9 quantify diffusional restrictions in DAAO immobilizates.<sup>33</sup>

10 In this work, D-Amino acid oxidase was genetically modified by fusion to an  
11 elastin-like polypeptide (ELP). Elastin-like polypeptides ELPs undergo a sharp and  
12 reversible phase transition at a specific temperature, thus ELP-DAAO was purified  
13 through phase transition, which has been demonstrated to be an efficient and simple  
14 way for purifying the DAAO. Multi-walled carbon nanotubes (MWCNTs) were  
15 selected as the model support to immobilize DAAO. Mora et al. studied the  
16 interaction of DAAO with single-walled CNTs for preparation of biosensors by  
17 adsorption of the enzyme on SWCNTs.<sup>17</sup> Herein we will demonstrate a novel  
18 approach for immobilization of DAAO on MWCNTs, as illustrated in scheme 1.  
19 MWCNTs were functionalized with hematin, and ELP-DAAO was specifically  
20 immobilized on the hematin-functionalized CNTs (hematin-CNTs), with the enzyme  
21 in proximity to the hematin. The ELP-DAAO/hematin-CNTs conjugate sequentially  
22 catalyzes the deamination of D-alanine and the decomposition of the evolved H<sub>2</sub>O<sub>2</sub>,  
23 mimicking multi-enzyme catalysis. The deterioration and inhibition effect by  
24 hydrogen peroxide can be significantly reduced, and molecular oxygen can be  
25 efficiently utilized to reoxidize the FAD factor. The methodology for highly specific

- 1 immobilization of enzyme is not restricted to the support carbon nanotubes, it can be
- 2 easily extended to other micro and nanomaterials for immobilization of oxidases, such
- 3 L-amino acid oxidase and glucose oxidase.



4  
5 **Scheme 1. Schematic presentation of procedures for specific immobilization of**  
6 **ELP-DAAO on the hematin-functionalized CNTs.**

7 CNTs were coated with MPTS, hematin was conjugated through the reaction between the sulfhydryl and  
8 alkene groups. ELP-DAAO was specifically immobilized through amidation reaction. The substrate  
9 D-alanine was converted to pyruvic acid catalyzed by the immobilized ELP-DAAO. The hematin  
10 catalyzed the decomposition of the generated hydrogen peroxide, and the evolved oxygen was recycled  
11 to oxidize the reduced cofactor FAD of DAAO. The forming of  $\text{H}_2\text{O}_2 \rightarrow \text{O}_2 \rightarrow \text{H}_2\text{O}_2$  circle is a driving  
12 force to accelerate the deamination reaction

13

## 1 **Experimental methods**

2 *Materials.* Restriction enzymes, DNA polymerase and DNA ligase were obtained  
3 from New England Biolabs and Fermentas. PCR and ligation products were separated  
4 and identified by gel electrophoresis (1% agarose) with appropriate DNA ladder and  
5 extracted using an extraction kit (OMEGA). SDS-PAGE analysis was performed on  
6 12% polyacrylamide gels. Oligonucleotide primers were synthesized by BGI Tech  
7 (Shenzhen, China). *E. coli* (*Escherichia coli*) strain DH5 $\alpha$  was used as a host for DNA  
8 manipulation, and the strain BL21 (DE3) was used as a host for the production of  
9 elastin-like polypeptides and enzymes. Multi-walled carbon nanotubes (MWCNTs)  
10 were purchased from Nanotech Port Co., Ltd (Shenzhen, China). The purity is higher  
11 than 95%, and the catalyst residue is less than 0.2 %. All other reagents were  
12 purchased from Sinopharm Chemical Reagent Co., Ltd (Shanghai, China) or  
13 Sigma-Aldrich (Shanghai, China) and used without additional purification processes.  
14 Double-distilled water was used in making solutions. Gene constructions and cloning  
15 for an elastin-like polypeptide (ELP) and expression vector construction have been  
16 described in supporting materials.

17 *Protein purification.* Proteins were purified using inverse transition cycling.<sup>34</sup>  
18 *E.coli* cells were harvested by centrifugation at 4 °C and resuspended in 50 mL of PBS  
19 buffer. Cells were lysed by ultrasonic disruption on ice, and the lysate was centrifuged  
20 at 10,000g at 4 °C for 30 min to remove cell debris. The supernatant was transferred  
21 to a fresh tube, and sodium chloride solution (3 M) was added and mixed with the  
22 sample. The resulting sample was heated to 30 °C for 10 minutes followed by  
23 centrifugation at 30 °C for 10 minutes. The purification process was repeated three  
24 times.

25 *Functionalization of carbon nanotubes with hematin.* 100 mg of purified

1 MWCNTs were dispersed in 20 ml of ethanol under sonication for 15 min. 3 ml of  
2 ammonia solution and 100 mg of 3-mercaptopropyltriethoxysilane (MPTS) were then  
3 added to the mixture and sonicated at 50 °C for 4 h. MPTS-coated CNTs  
4 (MPTS-CNTs) were finally obtained by filtering the solution through a polycarbonate  
5 membrane (0.2 μm), rinsing thoroughly with ethanol and subsequently with water.

6 100 mg of MPTS-CNTs were dispersed in 50 ml of DMSO under sonication for 30  
7 min, and then 20 mg of hematin and 20 mg of azobisisobutyronitrile (AIBN) were  
8 added. The mixture was incubated under shaking (200 rpm) at 60 °C for 12 h. The  
9 solution was then filtered through a polycarbonate membrane (0.2 μm), rinsed  
10 thoroughly with DMSO and subsequently with water. The samples were lyophilized.

11 The Ellman method<sup>35</sup> was adopted to determine the amount of SH groups. The  
12 Ellman agent is 5,5'-Dithiobis(2-nitrobenzoic Acid) (DTNB). According to the Ellman  
13 method<sup>35</sup>, 3-mercaptopropionic acid was used to react with DTNB. By measuring the  
14 adsorption at 412 nm, the standard curve for SH groups was obtained as shown in Fig.  
15 S1.

16 10 mg of MPTS-coated CNTs were dispersed in 3 ml of water by sonication for 5  
17 min, and then 0.1 ml DTNB solution (4.0 mg/ml, pH 8, 0.1M PBS) was added. After  
18 5 min of the Ellman reaction, the solution was filtered to remove the MPTS-coated  
19 CNTs, and the adsorption at 412 nm was measured for the filtrate. The standard curve  
20 for hematin is shown in Fig. S2. By detecting the hematin in the original hematin  
21 solutions and washing solutions after reaction, the amount of hematin immobilized on  
22 the MPTS-coated CNTs was determined to be  $0.109 \pm 0.003$  mg hematin/mg  
23 MPTS-coated CNTs.

24 *Enzyme immobilization.* The covalent attachment of ELP-DAAO onto the  
25 hematin-functionalized CNTs (hematin-CNTs) was based on the method previously

1 described.<sup>36</sup> Briefly, 200 mg of hematin-CNTs was dispersed in 200 mL of MES  
2 buffer (50 mM, pH 6.2), and then the mixture was added to a solution of NHS in MES  
3 buffer. The mixture was sonicated for 15 min, followed by addition of EDC (20  
4 mmol/L). The resulting mixture was shaken at 200 rpm for 1 h. The activated  
5 hematin-CNTs solutions were then filtered through a polycarbonate membrane (0.45  
6  $\mu\text{m}$ ) and rinsed thoroughly with MES buffer to remove excess EDC and NHS. The  
7 filtered hematin-CNTs were transferred to the ELP-DAAO solutions (4.0 mg/mL) and  
8 sonicated to redisperse the hematin-CNTs. The mixtures were then shaken (150 rpm)  
9 at 4 °C for 10 h. The mixtures were then centrifuged (4 °C) for 10 min at 7000g and  
10 the supernatants were removed. Typically, six washes were performed, with fresh  
11 buffer added each time to remove unbound ELP-DAAO. The concentrations of  
12 ELP-DAAO in the solutions were determined using the micro bicinchoninic acid  
13 (BCA) assay, as described in our previous work.<sup>37</sup> By detecting the protein in the  
14 original ELP-DAAO solutions, supernatants, and washing solutions after  
15 immobilization, the amount of ELP-DAAO immobilized on the hematin-CNTs was  
16 determined. Average values were obtained from triplicate measurements of three  
17 immobilization operations. The amount of ELP-DAAO immobilized was finally  
18 determined to be  $0.32 \pm 0.01$  mg ELP-DAAO/mg hematin-CNTs.

19 *Enzyme assay and analyses.* The enzyme activity was assayed at 30 °C. Free or  
20 immobilized ELP-DAAO was dissolved in a PBS buffer (50 mM, pH 8.0) with a  
21 concentration of 0.27 mg/mL. Protein concentration was measured by the BCA  
22 method.<sup>37</sup> The D-alanine concentrations were ranged from 15 to 80 mM, which were  
23 determined by HPLC. Kinetic parameters were determined by fitting the Michaelis–  
24 Menten equation to the initial rates, and substrate specificity and catalytic efficiency  
25 were calculated based on the parameters. At a relatively large scale (100 ml),

1 consecutive use of the immobilized enzyme was investigated. The substrate  
2 concentration was 100 mM, the enzyme concentration was 0.5 mg/ml, and the  
3 reactions were carried out 100 ml of PBS buffer (50 mM, pH 8.0). For each batch of  
4 immobilized enzyme, the catalysis was carried out at a constant temperature of 40 °C.  
5 The reaction time employed for each cycle was 6 h.

6 *X-ray photoelectron spectroscopy.* XPS spectra were acquired using a Thermo VG  
7 ESCALAB250 X-ray photoelectron spectrometer, which was operated at the pressure  
8 of  $2 \times 10^{-9}$  Pa using Mg Ka X-ray as the excitation source. Analysis of the data was  
9 carried out with Thermo Advantage XPS software.

10 *FTIR spectra measurement.* Infrared spectra for the samples were collected using a  
11 Fourier transform infrared (FTIR) spectrometer (Bruker TENSOR 27) equipped with  
12 a horizontal, temperature-controlled attenuated total reflectance (ATR) with ZnSe  
13 Crystal (Pike Technology). Infrared spectra were collected using a  
14 liquid-nitrogen-cooled mercury- cadmium- telluride detector that collected 128 scans  
15 per spectrum at a resolution of  $2 \text{ cm}^{-1}$ . All spectra were corrected by a background  
16 subtraction of the ATR element spectrum. Ultrapure nitrogen gas was introduced at a  
17 controlled flow rate to purge water vapor.

## 18 **Results and discussion**

19 *Expression and purification of recombinant D-amino acids oxidase.* By employing  
20 recombination cloning, the genes coding for DAAO and an elastin-like polypeptide  
21 (ELP) were joined. The fusion protein ELP-DAAO was expressed in *Escherichia coli*.  
22 Elastin-like polypeptides are artificial polypeptides.<sup>34</sup> ELPs undergo a sharp and  
23 reversible phase transition at a specific temperature. This property has been utilized to  
24 separate and purify proteins from fermentation broth.<sup>38</sup> Herein, ELP-DAAO was  
25 purified by using inverse transition cycling method using NaCl to trigger the phase

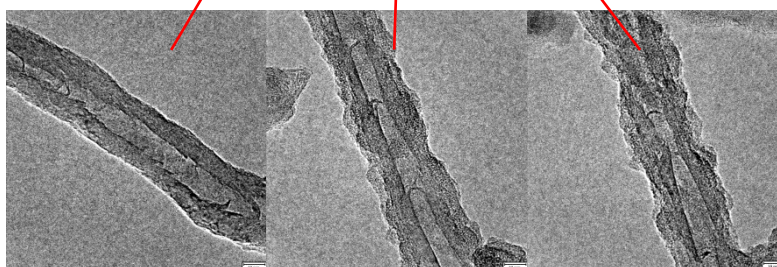
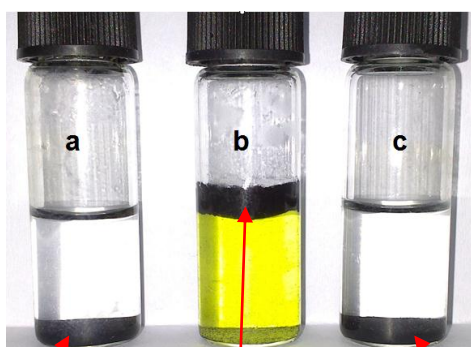
1 transition at 30 °C.<sup>34</sup> ELP-DAAO from the induced cultures was analyzed by 12%  
2 SDS-PAGE and visualized by Coomassie blue staining. A prominent protein band  
3 was clearly observed (Fig. S3, see supporting information), showing that ELP-DAAO  
4 was approximately 65.3 kDa in size, in agreement with the theoretically predicted  
5 molecular weight. After three successive rounds of inverse transition cycling,  
6 ELP-DAAO was purified that the contaminants were significantly decreased to a  
7 negligible level (Fig. S3, see supporting information).

8 *Specific immobilization of ELP-DAAO.* Scheme 1 shows the procedures for the  
9 specific immobilization of ELP-DAAO on the hematin-functionalized MWCNTs.  
10 Purified MWCNTs were coated with 3-mercaptopropyltriethoxysilane (MPTS)  
11 conferring sulfhydryl groups on their surfaces. Compared to the purified MWCNT (Fig.  
12 1a), the MPTS-coated MWCNT (Fig. 1b) shows a covered layer of MPTS with a  
13 rough surface. Purified MWCNTs precipitated at the bottom of the solution (Fig. 1a),  
14 while MPTS-coated MWCNTs floated on the top of the solution (Fig.1b) because of  
15 the density difference (MPTS, 0.987 g/cm<sup>3</sup>). When adding  
16 5,5'-Dithiobis(2-nitrobenzoic Acid) (DTNB) to the test tube, the solution become  
17 yellow (Fig.1b), due to the reaction of DTNB with the sulfhydryl groups.<sup>39</sup> The coating  
18 of MWCNTs by MPTS was also confirmed by the FTIR spectra as illustrated in Fig.  
19 2a. The two intense bands at 1096 and 1030 cm<sup>-1</sup> were assigned to Si-O-Si  
20 asymmetric stretching and Si-O-C, respectively, they are the characteristic bands of  
21 MPTS.<sup>40</sup> This is consistent with the results of X-ray photoelectron spectroscopy (XPS)  
22 (Fig. 2b). Compared to that of purified MWCNTs, the XPS spectrum for  
23 MPTS-coated MWCNTs exhibited bands for sulphur and silicon elements, they are  
24 from the MPTS (Fig. 1b), indicating that the MWCNTs have been coated with MPTS.

25 Through the reactions between the sulfhydryl groups of MPTS and the alkene

1 groups of hematin, as illustrated in Scheme 1, the CNTs were functionalized with  
2 hematin. After grafting hematin, the conjugate precipitated at the bottom of the  
3 solution (Fig. 1c), this is ascribed to the larger density of hematin ( $7.87 \text{ g/cm}^3$ ). When  
4 adding DTNB to the solution of hematin-MPTS-CNTs, the solution did not become  
5 yellow, indicating that the sulfydryl groups had reacted with the hematin, no sulfydryl  
6 groups were available to react with DTNB. The FTIR spectrum (the line in olive in  
7 Fig. 2a) is for the conjugate after grafting hematin. The band at  $1720 \text{ cm}^{-1}$  is due to  
8 C=O stretching vibrations of the carboxyl groups of hematin.<sup>41</sup> The XPS spectrum of  
9 hematin-MPTS-CNTs shows a band of nitrogen (the line in olive in Fig. 2b), which is  
10 from the hematin.

11



12

13

14

15

**Fig. 1. Carbon nanotube solutions and TEM images**

(a) Purified of MWCNTs; (b) MPTS-MWCNTs; (c) Hematin-MPTS-MWCNTs.

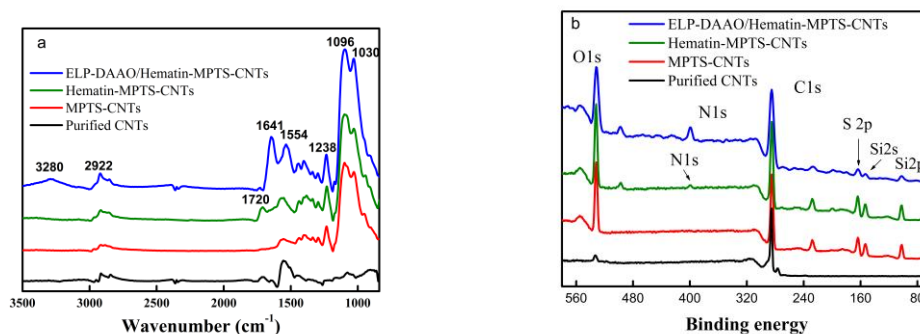


**Fig. 2. Spectra of FTIR (a) and XPS (b) for purified and functionalized CNTs**

Black: purified CNTs; red: MPTS-coated CNTs; Olive: hematin-functionalized CNTs; blue: ELP-DAAO immobilized CNTs

ELP-DAAO was specifically immobilized on the hematin-functionalized CNTs through amidation reactions (Scheme 1). The FTIR spectrum (the blue line in Fig. 2a) is for the conjugate after ELP-DAAO immobilization. The bands at  $1641\text{ cm}^{-1}$  and  $1554\text{ cm}^{-1}$  are due to amide I (C=O) and amide II (N-H), respectively.<sup>42</sup> On the other hand, the band at  $3280\text{ cm}^{-1}$  is attributed to hydroxyl groups from the protein. In the XPS spectrum of the conjugate with ELP-DAAO, the intensity of nitrogen is relatively increased (the blue line in Fig. 2b). This is attributed to the nitrogen atoms from the immobilized ELP-DAAO. The TEM image (Fig. 3a) shows that after the ELP-DAAO immobilization, the surface of the conjugate become much smooth compared to the rough surface of the hematin-functionalized CNTs (Fig. 1c). To further demonstrate the ability of hematin-functionalized CNTs for specific immobilization of proteins, the ELP was fused to green fluorescent protein (GFP), and ELP-GFP was immobilized on the hematin-functionalized CNTs. The ELP-GFP/hematin-CNTs conjugates were seen under optical microscope (DeltaVision OMX V3). ELP-GFP can be readily observed on the hematin-functionalized CNT (Fig. 3b). From the ELP-GFP spots, it can be known the distribution of immobilized ELP-GFP on the hematin-functionalized CNT.

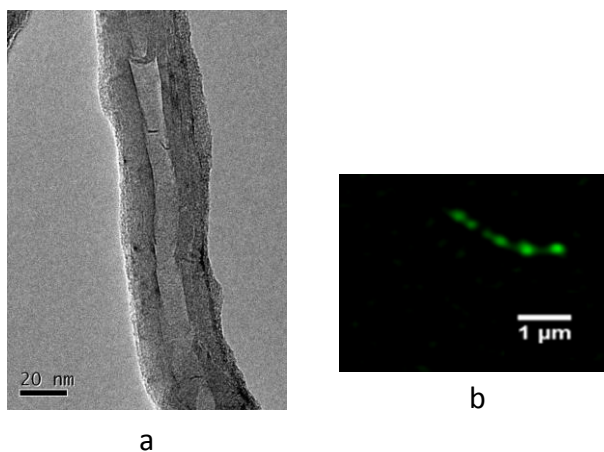


**Fig. 3. TEM (a) and optical (b) images**

a: ELP-DAAO/ hematin-functionalized CNT

b: ELP-GFP/ hematin-functionalized CNT

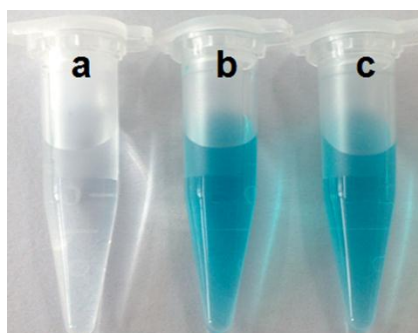
1

2

3

4

1 *Enzymatic activity for deamination of D-alanine.* Before evaluating the enzymatic  
2 activity, the ability of the hematin for decomposing hydrogen peroxide was tested.  
3 3,3',5,5'-Tetramethylbenzidine (TMB) was added to the test tubes. In the tube only  
4 containing TMB and hydrogen peroxide, due to very slow decomposition of hydrogen  
5 peroxide, the colour change of the solution was not obviously observed after 5 min  
6 reaction (Fig. 4a). In contrast, in the tubes containing the conjugates hemain-CNTs  
7 and ELP-DAAO/hemain-CNTs, due to the immediate decomposition of hydrogen  
8 peroxide by the hematin of the conjugates, TMB was oxidized and the solutions  
9 showed the typical blue colour (Fig. 4b and 4c).<sup>43</sup>



10  
11 **Fig. 4. Decomposition of hydrogen peroxide by hemain-CNTs (b)**  
12 **and ELP-DAAO/hemain-CNTs (c).**

13 Systems: (a) 100 mM H<sub>2</sub>O<sub>2</sub> + 0.5 mM TMB; (b) 20 μg/ml hematin-CNTs +100 mM H<sub>2</sub>O<sub>2</sub> +  
14 0.5 mM TMB; (C) 20 μg/ml ELP-DAAO/hemain-CNTs +100 mM H<sub>2</sub>O<sub>2</sub>+0.5 mM TMB.  
15 All the reactions were carried out in a PBS buffer (pH5.0) for 5 min. The conjugates in samples b and c  
16 were removed by centrifugation to see the colour more clearly.  
17

18 The reactions of D-alanine deamination were catalyzed by both the immobilized  
19 and free enzymes. An increase in the catalytic efficiency was observed using the  
20 immobilized ELP-DAAO when compared to the same amount of free ELP-DAAO in  
21 the solution. To observe the difference in the reactions catalyzed by free and  
22 immobilized enzymes, 2,4-dinitrophenylhydrazine (DNPH) was added to the tubes  
23 after reaction. DNPH can react with pyruvic acid and form a coloured product.<sup>45</sup> In  
24 the tube containing free ELP-DAAO (Fig. S4a), the solution exhibited a yellow colour;  
25 while in the tube containing immobilized ELP-DAAO (Fig. S4b), the solution

1 exhibited a red-brown colour. It is indicated that in the period of reaction time more  
 2 pyruvic acid was produced under the catalysis of the immobilized enzyme. The  
 3 difference in the colour change demonstrated that the immobilized ELP-DAAO  
 4 exhibited a much high catalysis efficiency than the free enzyme.

5 To study the enzyme kinetics, the activity of the immobilized ELP-DAAO was  
 6 compared to the activity of an equimolar free ELP-DAAO over a range of substrate  
 7 concentrations. The kinetic parameters are listed in Table 1. The  $V_{max}$  and  $K_m$  values  
 8 were determined by the Lineweaver–Burk plot derived from a series of experimental  
 9 determinations of the enzyme activity (Fig. S5). The kinetic parameters of the  
 10 immobilized enzyme were compared to that of the free enzymes. The free  
 11 ELP-DAAO exhibited a  $K_m$  value 234% times that of the immobilized enzyme. It  
 12 means that the immobilized enzyme has significantly improved the affinity towards  
 13 the substrate.<sup>44</sup> The  $K_{cat}/K_m$  ratio is a measure of the catalytic efficiency of enzymes  
 14 and has been used to compare the apparent kinetic parameters of the immobilized  
 15 enzyme.<sup>44</sup> The  $K_{cat}/K_m$  value of the immobilized ELP-DAAO is 324 % times that of  
 16 free ELP-DAAO, indicating a significant improvement of the enzyme catalytic  
 17 efficiency. Another parameter  $V_{max}/K_m$  is a measure of catalytic specificity.  
 18 Surprisingly, the catalytic specificity of the immobilized enzyme is more than 300%  
 19 times that of free ELP-DAAO. It is meant that the immobilized enzyme exhibited a  
 20 much higher catalytic specificity than the free enzyme. This is consistent with the  
 21 results shown in Fig. S4.

22 Table 1. Kinetic parameters for free and immobilized enzymes

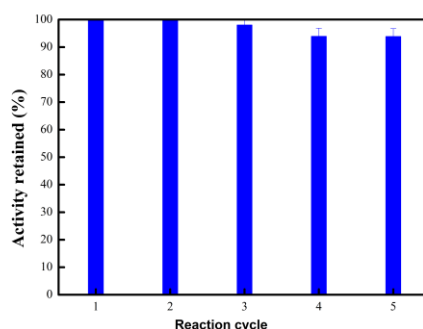
	Free ELP-DAAO	Immobilized ELP-DAAO
$V_m$ (mM.min <sup>-1</sup> )	0.107	0.148
$K_m$ (mM)	35.4	15.1
$K_{cat}$ (min <sup>-1</sup> )	26.0	36.0
$K_{cat}/K_m$ (min <sup>-1</sup> ·mM <sup>-1</sup> )	0.734	2.38

23

1 The enzymatic activity analysis showed that the activity of ELP-DAAO has been  
2 significantly improved through the specific immobilization. ELP-DAAO was  
3 immobilized in proximity to hematin to form the complex. The specific assembly of  
4 cooperating ELP-DAAO and hematin facilitated the control of the sequential catalysis  
5 process by coordinating the activities of ELP-DAAO and hematin. The hydrogen  
6 peroxide of DAAO was the substrate of hematin, and it was transferred from the  
7 active site of DAAO to the active site of hematin. Due to the molecular-distance  
8 proximity, the diffusion of the hydrogen peroxide into the bulk solution was reduced,  
9 and the hydrogen peroxide was immediately decomposed to water and oxygen. The  
10 intermediate decomposition of hydrogen peroxide led to that the concentration of  
11 oxygen in the local environment around the enzyme was increased, enabling efficient  
12 utilization of molecular oxygen ( $O_2$ ) for the oxidation of the reduced cofactor FDA of  
13 DAAO as illustrated in [Scheme 1](#). Maintaining the function of cofactors is important  
14 for enzymatic catalysis.<sup>46</sup> Thus the substrate D-alanine was converted in a high  
15 efficiency. The cooperation of the DAAO and hematin is a synergism which increases  
16 the productivity. In addition, the in situ decomposition of hydrogen peroxide can  
17 greatly reduce its potential deleterious effect on the immobilized DAAO, and  
18 significantly prevent the potential oxidation of production.<sup>47</sup>

19 The effect of pH on the activity retaining for free and immobilized enzymes is  
20 shown in [Fig. S6a](#). The optimal pH for the enzyme is around pH 8. As can be seen, at  
21 lower and higher pH values, the percentage of activity retained by the immobilized  
22 enzyme is much higher than that by the free enzyme. The effect of temperature on the  
23 activity retaining for free and immobilized enzymes is shown in [Fig. S6b](#). The optimal  
24 temperature for the free enzyme is at 30 °C, that for the immobilized enzyme is at 40  
25 °C. The temperature effect on the activity retaining for the immobilized is not

1 significant, while for the free enzyme, the change of activity retaining is relatively  
2 larger. Consecutive use of the immobilized enzyme was investigated as well. As can  
3 been in Fig.5, there was some decrease in the activity after five reaction/cleaning  
4 cycles, but not significant.



5  
6 **Fig. 5. Activity of immobilized enzyme after use in several consecutive cycles**

## 7 8 **Conclusions**

9 D-amino acid oxidase was genetically modified and the purification of the enzyme  
10 was performed in an efficient and simple way in a sustainable manner, with no  
11 pollutants taken into the process water. Highly specific immobilization of ELP-DAAO  
12 has been demonstrated. On the surface of the hematin-functionalized CNTs,  
13 ELP-DAAO is in proximity to the hematin at a molecular distance. This facilitates the  
14 transfer of the hydrogen peroxide from the active site of DAAO to the active site of  
15 hematin, and the hydrogen peroxide can be immediately converted with the catalysis  
16 of hematin. The local concentration of oxygen molecules around DAAO is much high  
17 compared to the bulk solution, and the molecular oxygen ( $O_2$ ) can be efficiently  
18 utilized to oxidize the reduced cofactor FDA of DAAO. The immobilized enzyme has  
19 a catalysis efficiency more than three times that of the free enzyme. The  
20 ELP-DAAO/hematin-CNTs conjugate showed the ability mimicking multi-enzyme  
21 complex system. The methodology for highly specific immobilization of enzyme is

1 not restricted to carbon nanotubes, and can be extended easily to other micro and  
2 nanomaterials as supports for specific immobilization of oxidases, such as glucose  
3 oxidase, nucleoside oxidase, monoamine oxidase, NADH oxidase, and xanthine  
4 oxidase, as illustrated in Fig. S7.

5 From environmental point of view, the presence of hydrogen peroxide in process  
6 water has caused the concerns of wastewater reuse. Industrial strength hydrogen  
7 peroxide is a strong oxidizer and as such requires special handling precautions.<sup>48</sup> In  
8 addition, hydrogen peroxide can interfere the analysis of chemical oxygen demand in  
9 wastewater.<sup>49</sup> Immobilization of catalase on the supports has been used to remove  
10 H<sub>2</sub>O<sub>2</sub> in order that process water can be returned to the environment.<sup>48,50</sup> The  
11 ELP-DAAO/hematin-CNTs conjugate can in situ decompose hydrogen peroxide  
12 evolved, eliminating the concerns of hydrogen peroxide presence in process water. In  
13 the process, ELP-DAAO was purified through an efficient and simple way in a  
14 sustainable manner, with no pollutants taken into the process water; the solvents used  
15 for the functionalization of carbon nanotubes were ethanol and DMSO, and the  
16 enzyme immobilization was performed in MES buffer. Ethanol,<sup>51-53</sup> DMSO,<sup>54-56</sup> and  
17 MES buffer<sup>57</sup> have been utilized as environmentally benign and green solvents. In  
18 addition, carbon nanotubes can be produced from a green process,<sup>58</sup> and the enzyme  
19 immobilized on carbon nanotubes can be easily recovered from the reaction media.<sup>36</sup>  
20 It can be concluded that the process from purification to specific immobilization of  
21 D-amino acid oxidase is green and environmentally benign.

## 22 Acknowledgements

23 This work was supported by the National Science Foundation of China (21376021,  
24 21176025), National Hi-tech R&D Program (2014AA022003), and the National Basic  
25 Research Program of China (2011CB200905).

1 **Reference**

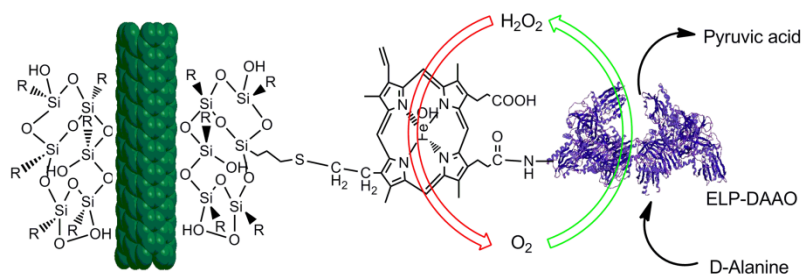
- 2 1. J. Y. Chung, E. T. Hwang, J. H. Kim, B. C. Kim and M. B. Gu, *Green Chem.*, 2014,  
3 **16**, 1163-1167.
- 4 2. F. H. Zhao, H. Li, Y. J. Jiang, X. C. Wang and X. D. Mu, *Green Chem.*, 2014, **16**,  
5 2558-2565.
- 6 3. L. Pollegioni, G. Molla, *Trends Biotechnol.*, 2011, **29**, 276-283.
- 7 4. S. Takahashi, M. Furukawara, K. Omae, N. Tadokoro, Y. Saito, K. Abe, Y. Kera,  
8 *Appl. Environ. Microbiol.*, 2014, **80**, 7219-7229.
- 9 5. S. Deng, E. Su, X. Ma, S. Yang, D. Wei, *Bioprocess Biosyst. Eng.*, 2014, **37**,  
10 1517-1526.
- 11 6. K. Yasukawa, S. Nakano, Y. Asano, *Angew Chem. Int. Ed.*, 2014, **53**, 4428-4431.
- 12 7. M. S. Pilone, S. Buto, L. Pollegioni, *Biotechnol Lett.*, 1995, **17**, 199-204.
- 13 8. K. Hernandez, A. Berenguer-Murcia, R. C. Rodrigues, R. Fernandez-Lafuente,  
14 *Current Organ. Chem.* 2012, **16**, 2652-2672.
- 15 9. R. Upadhyaya, S. G. Nagajyothi Bhat, *Biotechnol. Bioeng.*, 2000, **68**, 430-436.
- 16 10. R. Fernández-Lafuente, V. Rodriguez, J. M. Guisán, *Enzym. Microb. Technol.*,  
17 1998, **23**, 28-33.
- 18 11. E. M. Trost, L. Fischer, *J Mol Catal B: Enzym.*, 2002, **19**, 189-195.
- 19 12. B. Li, Z. Zhang, *Sens Actuators B: Chem.*, 2000, **69**, 70-74.
- 20 13. R. Domínguez, B. Serra, A. J. Reviejo, J. M. Pingarrón, *Analyt. Biochem.*, 2001,  
21 **298**, 275-282.
- 22 14. P. Pernot, J. P. Mothet, *Anal. Chem.*, 2008, **80**, 1589-1597.
- 23 15. Y. Inaba, K. Mizukami, N. Hamada-Sato, T. Kobayashi, C. Imada, E. Watanabe,  
24 *Biosens Bioelectron.*, 2003, **19**, 423-431.
- 25 16. E. Rosini, G. Molla, C. Rossetti, M. S. Pilone, L. Pollegioni, S. Sacchi, *J*

- 1 *Biotechnol.*, 2008, **135**, 377-384.
- 2 17. M. F. Mora, C. E. Giacomelli, C. D. Garcia, *Anal. Chem.*, 2009, **81**, 1016-1022.
- 3 18. D. Koszelewski, D. Pressnitz, D. Clay, W. Kroutil, *Org. Lett.*, 2009, **11**,
- 4 4810-4812.
- 5 19. Y. M. Seo, S. Mathew, H. S. Bea, T. H. Khang, S. H. Lee, B. G. Kim, H. Yun, *Org.*
- 6 *Biomol. Chem.*, 2012, **10**, 2482-2485.
- 7 20. Y. J. Chen, S. L. Goldberg, R. L. Hanson, W. L. Parker, I. Gill, T. P. Tully, M. A.
- 8 Montana, A. Goswami, R. N. Patel, *Org. Process Res. Dev.*, 2001, **15**, 241-248.
- 9 21. K. Parkin, H. O. Hultin, *Biotechnol. Bioengineer.*, 1979, **21**, 939-953.
- 10 22. F. López-Gallego, L. Betancor, C. Mateo, A. Hidalgo, N. Alonso-Morales, G.
- 11 Dellamora-Ortiz, J. M. Guisán, R. Fernández-Lafuente, *J. Biotechnol.*, 2005, **119**,
- 12 70-75.
- 13 23. Y. Zhao, Y. Zhu, J. Fu, *Appl. Surface Sci.*, 2014, **293**, 109-115.
- 14 24. M. Yoshimoto, M. Yamasaki, M. Okamoto, H. Umakoshi, R. Kuboi, *Enzym.*
- 15 *Microb. Technol.*, 2013, **52**, 13-19.
- 16 25. S. K. Mujawar, A. Kotha, C. R. Rajan, S. Ponrathnam, J. G. Shewale, *J.*
- 17 *Biotechnol.*, 1999, **75**, 11-22.
- 18 26. X. Mu, J. Qiao, L. Qi, Y. Liu, H. Ma, *ACS Appl. Mater. Interfaces*, 2014, **6**,
- 19 12979-12987.
- 20 27. J. M. Bolivar, B. Nidetzky, *Biotechnol. Bioengineer.*, 2012, **109**, 1490-1498.
- 21 28. K. S. Wong, W. P. Fong, P. Tsang, *Engineer Life Sci.*, 2011, **11**, 491-495.
- 22 29. E. Dey. Szwajcer, S. Flygare, K. Mosbach, *Appl. Biochem. Biotechnol.*, 1991, **27**,
- 23 239-250.
- 24 30. M. S. Pilone, L. Pollegioni, S. Buto. *Biotechnol. Appl. Biochem.*, 1992, **16**,
- 25 252-262.

- 1 31. R. Fernández-Lafuente, V. Rodríguez, C. Mateo, G. Fernández-Lorente, P.  
2 Arminsen, P. Sabuquillo, J. M. Guisán, *J. Mol. Catal. B: Enzym.*, 1999, **7**,  
3 173-179.
- 4 32. M. Yoshimoto, M. Okamoto, U. Ujihashi, T. Okita, *Langmuir*, 2014, **30**,  
5 6180-6186.
- 6 33. M. Leifheit, W. Bergmann, J. Greiser, *Eng. Life Sci.*, 2008, **8**, 540-545.
- 7 34. D. E. Meyer, A. Chilkoti, *Biomacromolecules*, 2002, **3**, 357-367.
- 8 35. G. L. Ellman, *Arch. Biochem. Biophys.* 1959, **82**, 70-77.
- 9 36. H. Tan, W. Feng, P. Ji, *Bioresource Technol.* 2012, **115**, 172-176.
- 10 37. J. Sun, K. Du, L. Fu, J. Gao, H. Y. Zhang, W. Feng, P. Ji, *ACS Appl. Mater.*  
11 *Interfaces*. 2014, **6**, 15132-15139.
- 12 38. M. R. Banki, L. Feng, D. W. Wood, *Nat. Methods*, 2005, **2**, 659-662.
- 13 39. R. Colman, R. Chu, *J. Biol. Chem.* 1970, 245, 606-615.
- 14 40. M. Minier, M. Salmain, N. Yacoubi, L. Barbes, C. Méhivier, S. Zanna, C. M.  
15 Pradier, *Langmuir*, 2005, **21**, 5957-5965.
- 16 41. R. Silverstein, G. Bassler, R. Morrill. *John Wiley & Sons: New York.*, 1981.
- 17 42. K. Du, J. Sun, X. Song, H. Chen, W. Feng, P. Ji, *ACS Sustainable Chem. Eng.* 2014,  
18 2, 1420-1428.
- 19 43. P. D. Josephy, T. Eling, R. P. Mason, *J. Biol. Chem.*, 1982, **257**, 3669-3675.
- 20 44. E. Sanfins, J. Dairou, S. Hussain, F. Busi, A. F. Chaffotte, F. Rodrigues-Lima  
21 and J. M. Dupret, *ACS Nano*, 2011, **5**, 4504-4511.
- 22 45. T. E. Friedemann And G. E. Haugen, *J. Biol. Chem.*, 1943, **147**, 415-442.
- 23 46. J. Rocha-Martín, B. L. Rivas, R. Muñoz, J. M. Guisán, F. López-Gallego,  
24 *ChemCatChem*, 2012, 4, 1279-1288.
- 25 47. J. Rocha-Martín, S. Velasco-Lozano, J. M. Guisán, F. López-Gallego. *Green*

- 1        *Chem.*, 2014, 16, 303-311.
- 2    48. D.S. Yoon, K. Won, Y.H. Kim, B.K. Song, S.J. Kim, S.J. Moon, B.S. Kim. *Water*  
3        *Sci Technol.*, 2007, **55**, 27-33.
- 4    49. T. Wu, J. D. Englehardt. *Environ. Sci. Technol.* 2012, **46**, 2291–2298
- 5    50. M. Alston, A. Willetts, A. Wells. *Org. Process Res. Dev.* 2002, **6**, 505-508
- 6    51. A. Laitinen, Y. Takebayashi, I. Kylänlahti, J. Yli-Kauhaluoma, T. Sugeta, K.  
7        Otake. *Green Chem.*, 2004, **6**, 49-52
- 8    52. L. Roumeas, C. Aouf, E. Dubreucq, H. Fulcrand. *Green Chem.*, 2013, 15,  
9        3268-3275.
- 10   53. B. Zhou, Z. C. Liu, W.W. Qu, R. Yang, X. R. Lin, S. J. Yan, J. Lin. *Green Chem.*,  
11        2014, **16**, 4359-4370
- 12   54. H. Chen, W. Dai, Y. Chen, Q. Xu, J. Chen, L. Yu, Y. Zhao, M. Ye, Y. Pan. *Green*  
13        *Chem.*, 2014, **16**, 2136-2141
- 14   55. I. Soroko, Y. Bhole, A. G. Livingston. *Green Chem.*, 2011, **13**, 162-168.
- 15   56. M. Martí, L. Molina, C. Alemán, E. Armelin. *ACS Sustainable Chem. Eng.*, 2013,  
16        **1**, 1609–1618
- 17   57. M. Taha, F. A. Silva, M. V. Quental, S. P. M. Ventura, M. G. Freire, J. A. P.  
18        Coutinho. *Green Chem.*, 2014, **16**, 3149-3159
- 19   58. S. Paul, S.K. Samdarshi, *New Carbon Materials.*, 2011, **26**, 85–88.
- 20

1 A table of contents entry



2

3 The specifically immobilized enzyme and hematin sequentially catalyze the conversion of D-alanine

4 and the decomposition of the generated hydrogen peroxide.